Insect Biochemistry and Molecular Biology 74 (2016) 68–75

Contents lists available at ScienceDirect

Insect Biochemistry and Molecular Biology

journal homepage: www.elsevier.com/locate/ibmb

Sequence variation determining stereochemistry of a Δ11 desaturase active in moth sex pheromone biosynthesis

Bao-Jian Ding*, Colm Carraher, Christer Löfstedt

Pheromone Group, Department of Biology, Lund University, Sölvegatan 37, SE-22362, Lund, Sweden

ARTICLE INFO

Article history:
Received 19 December 2015
Received in revised form
17 April 2016
Accepted 5 May 2016
Available online 6 May 2016

Keywords:
Desaturase
Stereochemistry
Di-iron center
Histidine rich motif
Mutagenesis
Moth pheromone evolution

ABSTRACT

A Δ11 desaturase from the oblique banded leaf roller moth *Choristoneura rosaceana* takes the saturated myristic acid and produces a mixture of (*E*)-11-tetradecenoate and (*Z*)-11-tetradecenoate with an excess of the Z isomer (35:65). A desaturase from the spotted fireworm moth *Choristoneura parallela* also operates on myristic acid substrate but produces almost pure (*E*)-11-tetradecenoate. The two desaturases share 92% amino acid identity and 97% amino acid similarity. There are 24 amino acids differing between these two desaturases. We constructed mutations at all of these positions to pinpoint the sites that determine the product stereochemistry. We demonstrated with a yeast functional assay that one amino acid at the cytosolic carboxyl terminus of the protein (258E) is critical for the *Z* activity of the *C. rosaceana* desaturase. Mutating the glutamic acid (E) into aspartic acid (D) transforms the *C. rosaceana* enzyme into a desaturase with *C. parallela*-like activity, whereas the reciprocal mutation of the *C. parallela* desaturase transformed it into an enzyme producing an intermediate 64:36 *E/Z* product ratio. We discuss the causal link between this amino acid change and the stereochemical properties of the desaturase and the role of desaturase mutations in pheromone evolution.

1. Introduction

The integral membrane fatty acyl desaturases (FADs) in the Lepidoptera have evolved to function not only in normal cellular lipid metabolism, but also in the biosynthesis of moth sex pheromones that are more or less species-specific chemical signals for mate recognition (Knipple et al., 2002). Desaturases are key enzymes producing the great diversity of moth pheromones (Knipple et al., 1998; Liu et al., 2002; Roelofs et al., 2002; Jeong et al., 2003; Liénard et al., 2010). They introduce double bonds at different locations in the fatty acyl chain in *E* or *Z* configurations. Most desaturases active in moth pheromone biosynthesis prefer 14–18C substrates (Liénard et al., 2008; Ding et al., 2011). Based on the position in which the double bond is introduced and their phylogenetic relationships, desaturases in Lepidoptera can be organized into different groups. Most of them fall into three major groups; a Δ9 (16C > 18C) clade with a preference for palmitic acid, a Δ9 (18C > 16C) with a preference for stearic acid, and a third clade comprising Δ11, Δ10, bifunctional desaturases and other desaturases (Roelofs et al., 2002; Löfstedt et al., 2016). The first two clades comprise mostly homeostatic desaturases, which are important for maintaining the fluidity of cell membranes, whereas the third clade contains desaturases mainly dedicated for pheromone production.

Some desaturases have evolved multiple functions that entail conjugated double bonds (Moto et al., 2004; Matoušková et al., 2007; Serra et al., 2006) and in some cases the same desaturase can produce a triple bond in the acyl chain of moth sex pheromones by sequential action (Serra et al., 2007). There are many desaturases reported that interact with the same substrate, but their products may have strikingly different stereochemistry and have a strong influence on species specificity of the sex pheromone (Hao et al., 2002; Liu et al., 2004; Buček et al., 2015). Different moth species often use specific ratios of *E* and *Z* isomers of their fatty acid-derived sex pheromones. These differences may be determined directly by the isomer ratios produced by the desaturases or they may be modulated by the subsequent action of fatty acyl reductases (FARs), critical in transforming the fatty acyl precursors into volatile pheromone components (Lassance et al., 2010; Liénard and Löfstedt, 2010).

A desaturase from *Choristoneura rosaceana* (CroΔ11, GenBank *accession no.* AF545481) operating on myristate produces a mixture

* Corresponding author.
E-mail address: bao-jian.ding@biol.lu.se (B.-J. Ding).

http://dx.doi.org/10.1016/j.ibmb.2016.05.002

of *E/Z*11-14:CoA in a ratio of 1:7 (Hao et al., 2002), whereas the desaturase from *Choristoneura parallela* (CpaE11, GenBank *accession no.* AF518014) also interacts with myristate but produces almost pure E11-14:CoA (Liu et al., 2004). In the present study we address the consequences of sequence variation for the stereochemical output of the activity of these desaturases. We constructed mutations of CroΔ11 based on the amino acids found to be different in comparison with CpaE11 to investigate the influence of these specific sites on the product specificity of the enzymes.

2. Materials and methods

2.1. Vector construction and mutagenesis

To construct a series of mutated CroΔ11 desaturases, the entry clone harboring the wild type CroΔ11 desaturase (synthesized by GeneArt, invitrogen) was used as a template. Two PCR fragments were generated for each target construct, by using the specific primers as shown in Table 1 and in combination with M13 forward and reverse primers (Atanassov et al., 2009). The two fragments containing the *attL1* site and *attL2* site (recombination sites for Gateway® technology) were cut from the agarose gel and purified using the Wizard® SV Gel and PCR Clean up system (Promega Biotech AB, Nacka, Sweden). Their concentration was measured by NanoDrop2000 (Thermo Scientific, Saveen Werner, Malmö, Sweden) and their mole amount was calculated, then a fusion PCR was performed by adding each of the two fragments in the same molar amount, along with PCR buffer, dNTP and phusion® Taq (Thermo Scientific), in a 20 μL reaction. Thermo cycle conditions were as follows: 98 °C 30 s, then 10 cycles of 98 °C 5 s, 72 °C 2 min, then the reaction was cooled quickly to 4 °C. Two μL of this fused product was taken to a new tube to be used as template for a new round of PCR reaction, with M13+ and M13− primers to amplify the successfully fused mutated genes. The PCR product was checked by electrophoresis on agarose gel and purified with the promega kit as before. The fragment was then cloned into pYEX-CHT-DEST by LR reaction (Atanassov et al., 2009), and recombinant constructs were analyzed by sequencing.

2.2. Yeast heterologous expression

The pYEX-CHT recombinant expression vectors containing the mutated desaturase gene were introduced into the double deficient *ole1 elo1* strain (*MATa elo1::HIS3 ole1::LEU2 ade2 his3 leu2 ura3*) of the yeast *Saccharomyces cerevisiae*, defective in both desaturase and elongase functions (Schneiter et al., 2000) using the *S.c.* easy yeast transformation kit (Life technologies). For selection of uracil and leucine prototrophs, the transformed yeast was allowed to grow on

Table 1
Primers used for mutagenesis.

Primer	Sequence
12LM	GTTGAGGATATGGAATCTGATATGCCTGAGAGCGAGGAAAAGC
12antisense	GCTTTTCCTCGCTCTCAGGCATATCAGATTCCATATCCTCAAC
16del_E	ATCTTCCTGAGAGCGAGAAGCTTGAGAAGCTTGT
16antisense	ACAAGCTTCTCAAGCTTCTCGCTCTCAGGAAGAT
19LW	CTTCCTGAGAGCGAGGAAAAGTGGGAGAAGCTTGTTGCTCCTCAA
19antisense	TTGAGGAGCAACAAGCTTCTCCCACTTTTCCTCGCTCTCAGGAAG
33QE	GCTGCTCCTAGAAAGTACGAGATTATCTACACCAACC
33antisense	GGTTGGTGTAGATAATCTCGTACTTTCTAGGAGCAGC
45WG	CTGCTGACCTTCGGTTACGGGCATATTGCTGGTC
45antisense	GACCAGCAATATGCCCGTAACCGAAGGTCAGCAG
65IV	CTGCTAAGTGGCAGACCGTTATTCTGGCTCTTATC
65antisense	GATAAGAGCCAGAATAACGGTCTGCCACTTAGCAG
69LI	CAGACCATTATTCTGGCTATTATCCTGAACGAGATGG
69antisense	CCATCTCGTTCAGGATAATAGCCAGAATAATGGTCTG
88AS	TGGTGCTCATAGGCTTTGGAGTCATAGATCTTACAAGGCT
88antisense	AGCCTTGTAAGATCTATGACTCCAAAGCCTATGAGCACCA
95TA	CATAGATCTTACAAGGCTGCTGTGCCTCTTCAGATCA
95antisense	TGATCTGAAGAGGCACAGCAGCCTTGTAAGATCTATG
103IM	CAGATCATCCTGATGATCTTCAACAGC
103antisense	GCTGTTGAAGATCATCAGGATGATCTG
109SA	ATCTTCAACAGCCTGGCTTTCCAGAACTCTGCT
109antisense	AGCAGAGTTCTGGAAAGCCAGGCTGTTGAAGAT
116HN118IV	GAGCTTCCAGAACTCTGCTATTAACTGGGTTAGGGATCATAG
116antisense	CTATGATCCCTAACCCAGTTAATAGCAGAGTTCTGGAAGCTC
161AG163TM	CCCTGAGGTTAAGAAGAGGGGTAAGATGATCGATATGAGCGATATCTA
161antisense	TAGATATCGCTCATATCGATCATCTTACCCCTCTTCTTAACCTCAGGG
174IV	GAGCGATATCTACTCTAACCCTGTCCTGAGGTTTC
174antisense	GAAACCTCAGGACAGGGTTAGAGTAGATATCGCTC
250MI251TA	TGCCTGCTGAGAACAAGATAGCCTTAATTGCTTGCCTTGGTGAGA
250antisense	TCTCACCAAGGCAAGCAATTAAGGCTATCTTGTTCTCAGCAGGCA
252FL	TGAGAACAAGATGACCTTAATTGCTTGCCTTGGTGAG
252antisense	CTCACCAAGGCAAGCAATTAAGGTCATCTTGTTCTCA
258ED	TCATTGCTTGCCTTGGTGATAGCTTCCACAACTACCACCAT
258antisense	ATGGTGGTAGTTGTGGAAGCTATCACCAAGGCAAGCAATGA
259NS	GCTTGCCTTGGTGAGAGCTTCCACAACTACCAC
259antisense	GTGGTAGTTGTGGAAGCTCTCACCAAGGCAAGC
286KQ	TCGGAATGAATTGGACCGCTCAGTTCATCGATTTCTTC
286antisense	GAAGAAATCGATGAACTGAGCGGTCCAATTCATTCCGA
309KN	ACTGCTTCCGATGAGAACATCAATAGCAGGATGAAG
309antisense	CTTCATCCTGCTATTGATGTTCTCATCGGAAGCAGT
321VI	GAAGAGAACCGGTGATGGTACTGATATAAGCGGTCAAAAGTAT
321antisense	ATACTTTTGACCGCTTATATCAGTACCATCACCGGTTCTCTTC

SC plates containing 0.7% YNB (w/o amino acid, with ammonium sulfate) and a complete drop-out medium lacking uracil and leucine (Formedium™ LTD, Norwich, England), 2% glucose, 1% tergitol (type Nonidet NP-40, Sigma-Aldrich Sweden AB, Stockholm, Sweden), 0.01% adenine (Sigma) and 0.5 mM oleic acid (Sigma) as an extra fatty acid source.

After 4 days incubation at 30 °C, individual colonies were picked to inoculate 10 mL selective medium and then grown at 30 °C and 300 r.p.m for 48 h. Yeast cultures were diluted to an OD_{600} of 0.4 in 20 mL fresh selective medium containing 2 mM $CuSO_4$ with supplementation of the biosynthetic precursor, i.e. the methyl myristate (14:Me) (Larodan Fine Chemicals, Malmö, Sweden). The FAME precursor was prepared at a concentration of 100 mM in 96% ethanol and added to reach a final concentration of 0.5 mM in the culture medium (Ding et al., 2011). Yeasts were cultured at 30 °C with Cu^{2+}-induction.

After 48 h yeast cells were harvested by centrifugation at 3000*g* and the medium was discarded. Total lipids were extracted using 3.75 mL of methanol/chloroform (2:1, v/v), in a glass tube. One mL of acetic acid (0.15 M) and 1.25 mL of water were added to the tube to wash the chloroform phase. Tubes were vortexed vigorously and centrifuged at 2000*g* for 2 min. The bottom chloroform phase, about 1 mL, containing the total lipids, was transferred to a new glass tube. Fatty acid methyl esters (FAMEs) were made from this total lipid extract by acid methanolysis. One mL of 2% sulfuric acid in methanol (v/v) was added to the tube, vortexed vigorously, and incubated at 90 °C for 1 h. After incubation, 1 mL of water was added and mixed well, and then 1 mL of hexane was used to extract the FAMEs.

2.3. GC-MS analysis of fatty acids

The methyl ester samples were subjected to GC-MS analyses on a Hewlett Packard 6890 GC coupled to a mass selective detector HP 5973. The GC was equipped with an INNOWax column (30 m × 0.25 mm × 0.25 μm), and helium was used as the carrier gas (average velocity: 33 cm/s). The MS was operated in electron impact mode (70 eV), and the injector was configured in splitless mode at 220 °C. The oven temperature was set to 80 °C for 1 min, then increased at a rate of 10 °C/min up to 210 °C, followed by a hold at 210 °C for 15 min, and then increased at a rate of 10 °C/min up to 230 °C followed by a hold at 230 °C for 20 min. The monounsaturated fatty-acid products were identified by comparing their retention times and mass spectra with those of synthetic standards. The double bond positions were further confirmed by DMDS derivatization (Buser et al., 1983) and subsequent GC-MS analysis. FAMEs (50 μL) were transferred to a new tube, 50 μL DMDS was added and the mixture was incubated at 40 °C overnight, in the presence of 5 μL of iodine (5% in diethyl ether). Hexane (200 μL) was added to the sample and the reaction was neutralized by addition of 50–100 μL $Na_2S_2O_3$ (15% w/v in water). The organic phase was recovered and concentrated under a gentle nitrogen stream to a suitable volume. DMDS derivatives were analyzed on an Agilent 6890 GC system equipped with an HP-5MS capillary column (30 m × 0.25 mm × 0.25 μm, Agilent) coupled with an HP 5973 mass selective detector. The oven temperature was set at 80 °C for 1 min, raised to 140 °C at a rate of 20 °C/min, then to 250 °C at a rate of 4 °C/min and held for 20 min (Wang et al., 2010).

2.4. Desaturase modeling

The membrane topology of the moth desaturases was constructed based on TMHMM prediction (Krogh et al., 2001) and the desaturase models published previously (Libisch et al., 2000; Gagné et al., 2009; Vanhercke et al., 2011; Meesapyodsuk et al., 2007; Man et al., 2006). 3D structural models were constructed with SWISS-MODEL (http://swissmodel.expasy.org) based on the 3D structure of mSCD1 (Bai et al., 2015) and hSCD1 (Wang et al., 2015). Docking analyses of the substrate myristic acid-CoA were carried out with Autodock Vina (Trott and Olson, 2010).

3. Results and discussion

By comparing the amino acid sequence of CroΔ11 and CpaE11, we found differences to be restricted to 24 amino acids (Fig. 1), although the stereochemical output – i.e. the E to Z isomer product ratio of the two enzymes – is very different. In order to pinpoint the site(s) that control the product stereochemistry of the CroΔ11 desaturase, a series of mutated versions of CroΔ11 were created by fusion PCR and Gateway™ methods. All in all 21 mutations were performed, three of them containing two neighbouring amino acid changes (i.e. 116 + 118, 161 + 163, 250 + 251) and the remaining containing one amino acid change only. The mutated constructs were confirmed by sequencing and subsequently used to transform the yeast strain deficient in both desaturase and elongase (*ole1/elo1*). The yeast transformants were cultured in the presence of methyl myristate supplemented as substrate and the yeast fatty acid composition was analyzed. It was shown that when exchanging the amino acid at the sites in Fig. 1, from CroΔ11 to their counterpart in CpaE11, in most of the cases, the catalytic activity was not affected at all (Table 2). In two cases (Q33E and S109A), the enzyme activity was totally disrupted; possibly because the changes interrupt the substrate binding motif of the enzyme, as the asparagines (N) following positions 38 and 112 (corresponding to 75 and 148 in hSCD1) are important substrate binding residues of the enzyme (Wang et al., 2015). When another site, at position 258, located near the third histidine rich motif, was changed from E to D (from glutamic to aspartic acid), the *Z* activity decreased dramatically (Fig. 2), thus affecting the stereochemical output. This mutant was assayed in several replicates, confirming the result. When the reciprocal mutation of the 258D in CpaE11 to E was assayed, it was found to bestow CpaE11 with *Z* activity (Table 3, Fig. 3). Our interpretation is that the glutamic acid at position 258 is critical for the *Z* activity of CroΔ11. We observed that the CroΔ11_E258D mutant did not completely abolish the Z activity of the enzyme, and likewise, the CpaE11_D258E mutant did not completely modify the Z ratio of the products to the level of the wild type CroΔ11. This suggests that there are other amino acids influencing the stereochemical specificity of desaturase besides 258E/D. The amino acid at position 258 is among several residues that form the secondary coordination sphere of the dimetal unit (Bai et al., 2015) (Figs. 4 and 5), all of which are likely to have an influence on the enzymatic activity of the desaturase.

Desaturases that catalyze the introduction of double bonds into fatty acyl chains form two distinct classes, however, they all require molecular oxygen and an electron donor, mostly cytochrome b_5 (Okuley et al., 1994). One group is formed by soluble desaturases operating on substrate acyl-acyl carrier protein (ACP) complexes, found in plants and localized in plastids (Lindqvist et al., 1996), and usually introduce the first double bond in a saturated molecule (Los and Murata, 1998; Knipple et al., 1998). The other group, including the majority of fatty acid desaturases (FADs), are membrane-bound desaturases recognizing acyl chains esterified to CoA or phospholipids, and they are involved in biosynthesis of (poly)unsaturated fatty acids (Tocher et al., 1998). These desaturases are characterized by possessing three histidine rich motifs, all on the same side of the membrane, and four to six membrane-spanning helices (Sperling et al., 2003). The two groups are completely unrelated although they use the same cofactors and act similarly regarding product stereochemistry (Shanklin and Cahoon, 1998; Sperling et al., 2003).

Fig. 1. Sequence alignment of CroΔ11 and CpaE11 with the mammalian SCD1s. Identity and similarity between the two insect desaturases were, 311/335 (92%) and 326/335 (97%) respectively. Magenta font represents amino acids in the cytosol, turquoise amino acids are in the ER lumen and the black amino acids anchor in the ER membrane (transmembrane), as predicted by TMHMM Server v. 2.0. The boxes in the alignment are the sites at which mutations were performed. Histidine boxes are shown as underlined. Key residues involved in substrate binding are labeled with solid balls and the amino acid position 258 is indicated with a star.

The alkane hydroxylases, acetylenases, epoxygenases, and even the enzymes that catalyze the postulated decarbonylation of aldehydes are all variations of the membrane-bound desaturases (Shanklin et al., 1994; Sperling et al., 2003). They all house a di-iron complex, and are evolutionarily very close to each other. Evidence to support this close relationship includes the fact that as few as four amino acid substitutions can convert a Δ12 desaturase to a hydroxylase and as few as six result in conversion of a hydroxylase to a desaturase, reflecting the catalytic plasticity of fatty acid modification enzymes (Broun et al., 1998). This has led to a wide range of studies using mutagenesis to investigate the functional aspects of desaturases, linking regioselectivity, substrate specificity, and chemoselectivity (desaturation/acetylenation ratio), to a defined region or motif of the desaturase sequences (Vanhercke et al., 2011; Gagné et al., 2009; Meesapyodsuk et al., 2007).

The recently determined 3D structure of membrane bound acyl-CoA desaturases mSCD1 (Bai et al., 2015) and hSCD1 (Wang et al., 2015) provide a detailed explanation of the structure-function relationships of membrane–bound fatty acid desaturases; along with the crystal structures of the castor and the English ivy soluble ACP-desaturases (Lindqvist et al., 1996; Guy et al., 2007) which already provided some insights for engineering desaturases with novel

Table 2
The E/Z isomer ratios produced by mutated CroΔ11 compared with wild type CroΔ11. In CroQ33E and CroS109A, the enzyme activity was totally disrupted.

Mutations	E11-14:CoA/Z11-14:CoA
CroΔ11_wt	35:65
CroL12M	31:69
Cro16del_E	33:67
CroL19W	34:66
CroQ33E	–
CroW45G	31:69
CroI65V	35:65
CroL69I	30:70
CroA88S	32:68
CroT95A	35:65
CroI103M	36:64
CroS109A	–
CroH116N_I118V	42:58
CroA161G_T163M	36:64
CroI174V	35:65
CroM250I_T251A	35:65
CroF252L	33:67
CroE258D	86:14
CroN259S	31:69
CroK286Q	35:65
CroK309N	34:66
CroV321I	35:65

Table 3
The E/Z isomer ratios produced by mutated CroΔ11 and CpaE11 compared with their wild type counterparts. N = 5, (±SEM).

Reciprocal mutations	E11-14:CoA/Z11-14:CoA
CroΔ11_wt	35:65 (±1.4)
CroΔ11E258D	91:9 (±1.5)
CpaE11_wt	99:1 (±0.13)
CpaE11D258E	64:36 (±3.7)

catalytic activities and specificities (Cahoon et al., 1997; Guy et al., 2006; Whittle et al., 2008). The majority of fatty acid desaturase mutagenesis studies are based on mapping onto a topological model as shown in Fig. 4. Our model is constructed in light of several models described in various studies (Libisch et al., 2000; Gagné et al., 2009; Vanhercke et al., 2011; Meesapyodsuk et al., 2007; Man et al., 2006). Consistent with the structure of mSCD1, TM2 and TM4 have a few amino acids that protrude out of the membrane and provide some of the coordinating residues for the di-iron active site (Bai et al., 2015). The residues 95–116 form a helix similar to helix 1 in SCD1 that is amphipathic and probably resides at the interface between the cytosolic domain and the lipid bilayer.

Many endeavors have been made to address the different functional aspects of desaturases. By constructing the chimeric *Boofd6* desaturase, Libisch et al. (2000) found that chain length specificity is determined by transmembrane helices 1 and 2 that are involved in forming the substrate-binding site. Meesapyodsuk et al. (2007) showed that two amino acids in the C-terminus determined the ratio of Δ15/Δ12 products of CpDesX from *Claviceps purpurea*, providing some insights into the nature of regioselectivity of this desaturase. Recently, swapping of a single amino acid (A224I) in the fatty acyl substrate binding tunnel introduced E/Z14-desaturation activity to MsexD2 which is a desaturase already exhibiting Z11-desaturation and conjugation activity (Matoušková et al., 2007; Buček et al., 2015). This study lead to the identification of a minimal structural motif that can bestow new desaturation activity and hence underlined the inherent evolvability of pheromone biosynthetic FADs which can shape the moth pheromone composition.

Previously it was shown that the three histidine rich motifs (Fig. 4) are crucial for the catalytic activity of a desaturase (Shanklin et al., 1994; Haritos et al., 2014), mutation of any of these histidines disrupt the desaturase functionality, presumably disturbing the di-iron binding at the catalytic center. Even the amino acids flanking the histidine rich motifs are critical for the catalytic properties, as shown in the study of the plant FAD2 desaturase (Broun et al., 1998; Broadwater et al., 2002). They demonstrated that two amino acids, adjacent to the di-iron binding region, determine the product chain length distribution and reaction outcome. Moreover, by using random mutagenesis Vanhercke and colleagues found that a limited number of amino acid changes close to the membrane surface, can have a significant effect on the regioselectivity and chain length specificity of an acyl-CoA fatty acid desaturase (Vanhercke et al., 2011). These studies suggest that these scattered amino acids that are not involved in the formation of the membrane anchor may build up the catalytically active sites. A better understanding of the structure-function relationships of fatty acid desaturases would open up the possibility to manipulate the double bond position of substrates with various chain lengths to make novel and valuable fatty acids or fatty acid derivatives.

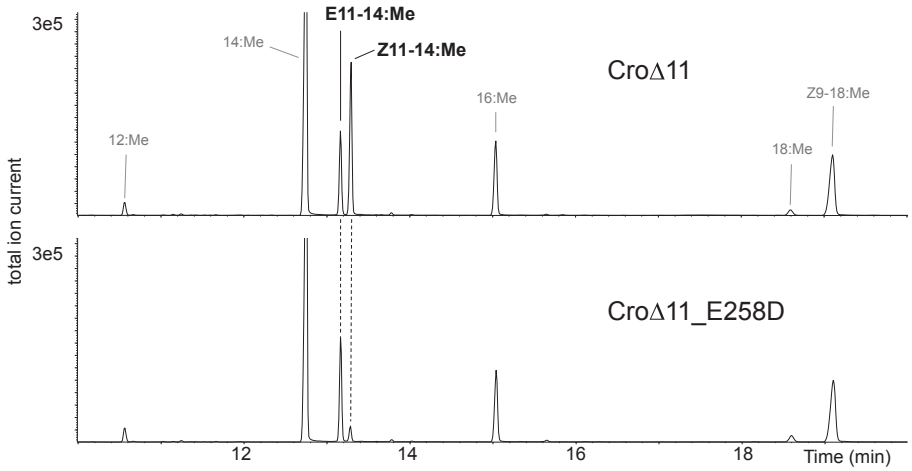

Fig. 2. Fatty acid methyl ester profiles from GC-MS analyses of yeast expressing the wild type CroΔ11 (upper trace) and the mutated CroΔ11_E258D (lower trace). The larger black font indicates methyl esters that are the product of the desaturase, and the smaller grey font indicates methyl esters that are supplemented to the yeast medium or naturally occurring in the yeast cells.

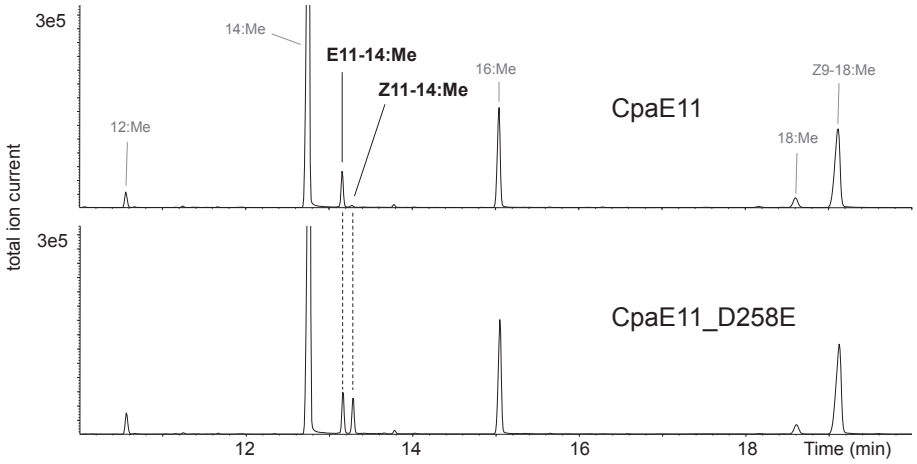

Fig. 3. Fatty acid methyl ester profiles from GC-MS analyses of yeast expressing the wild type CpaE11 (upper trace) and the mutated CpaE11_D258E (lower trace). The larger black font indicates methyl esters are the product of the desaturase, and the smaller grey font indicates methyl esters are supplemented to the yeast medium or naturally occurring in the yeast cells.

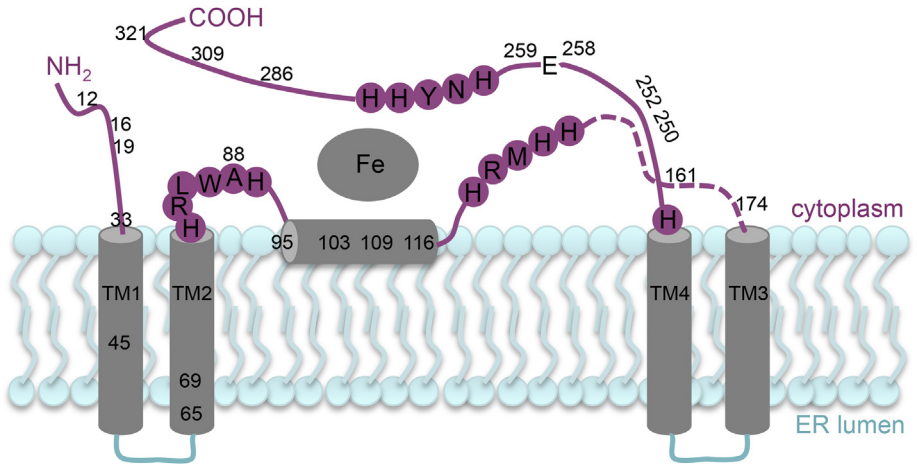

Fig. 4. Topological model of CroΔ11 desaturase spanning the ER membrane. The amino acids of the histidine-boxes in the cytosol, crucial for the catalytic activity of desaturase, are depicted as magenta circles. The numbers along the peptide chain indicate the positions of mutations made in this study.

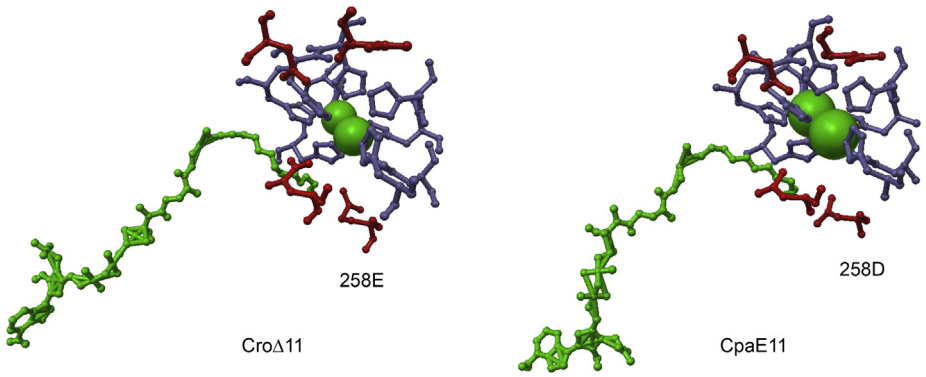

Fig. 5. Residues forming both the primary and secondary coordination shell around the dimetal center in CroΔ11 and CpaE11. Histidine residues (purple) are the first coordinating residues and the red residues are the secondary coordination residues. The metal ions are shown as green spheres. The aspartic acid, and glutamic acid at position 258 are labeled. The substrate myristic acid-CoA, shown docked at the highest scoring position according to Autodock Vina (Trott and Olson, 2010), is in green.

Regarding the stereochemistry of the desaturation product, the amino acids in the immediate neighborhood of the di-iron center determine the geometry and the size of the hydrophobic cavity (reactive cavity), which will affect the stereochemical outcome of

the reaction as proposed by a study on a Δ8 sphingolipid desaturase (Beckmann et al., 2002). This desaturase catalyzes the formation of both *Z*- and *E*- double bonds suggesting the active site cavity is large and flexible enough to bind the substrate in two alternative conformations, which results in the *Z*- or *E*- outcome respectively (Beckmann et al., 2002). Moreover, an insect derived palmitoyl-CoA Δ11 desaturase showed different catalytic behavior when given substrates of different chain length (Pinilla et al., 1999). With the increase of chain-length, the proportion of E-isomer decreased dramatically, suggesting that when the length of the overhanging alkyl residue is increased, the chance to accommodate two conformational isomers in the active site decreased.

The available sequence data do not yet allow recognition of the critical amino acids responsible for the differences in the stereochemical outcome of desaturase reactions. In the present study, we found an amino acid in the vicinity of the third histidine rich motif that contributes strongly to the *Z* activity of an insect-derived desaturase. Loss or gain of this amino acid results in loss or gain of *Z* isomer in the product output (Table 3). In the docking experiments (Fig. 5), the 258E/D residue is shown to contribute to the formation of the secondary coordination sphere of the dimetal unit, along with 129D, 133D and 228N. Thus, this residue could be influencing the shape of the reactive cavity and may play an important role in the catalytic property of this desaturase.

Chain length and double bond positional specificities of a soluble plant fatty acid desaturase have been studied in great detail (Cahoon et al., 1999). The amino acid contact residues in the substrate binding channel of the soluble fatty acid desaturase were identified, and subsequently replaced with different residues to modify the enzymes activity. But these residues are in most cases not transferable to the acyl-CoA type desaturases. Tyr104 on TM2 probably has a crucial role in determining the substrate length in mSCD1, because it is capping the end of the substrate tunnel (Bai et al., 2015). When the threonine at the corresponding position was changed to tyrosine, the *Calanus hyperboreus* desaturase (ChDes1) lost its ability to accept cerotic acid, while retaining the ability to desaturate 18:0 (Meesapyodsuk and Qiu, 2014). In our moth desaturases, CpaE11 and CroΔ11, the highly conserved Tyr is replaced by Asn, it would be interesting to change it back to Tyr to see how this affects the substrate chain length preference.

Our study demonstrates that one amino acid is critical for determining the stereochemical specificity of a Lepidopteran desaturase. This parallels a previous mutagenesis study addressing substrate preference of the fatty acyl reductase involved in pheromone biosynthesis (pgFAR) (Lassance et al., 2013) and further substantiates the idea that single amino acid polymorphisms may underlie drastic changes in pheromone composition. *E/Z* isomer ratios are important for the activity and species-specificity of moth sex pheromones (Löfstedt et al., 1991). The *E/Z* ratio produced by the desaturase may be subsequently modulated by the selectivity of the pgFAR (Lassance et al., 2010, 2013) but in many cases the stereochemistry of the desaturation may directly influence the *E/Z* ratio between the final pheromone components. Our results also demonstrate the potential for tailor-made production of specific insect pheromone components in cell and plant factories (Hagström et al., 2013; Ding et al., 2014) through protein engineering of the desaturases involved.

Acknowledgements

This study was supported by external grants from the Swedish research council (VR), the research council Formas, The Swedish Foundation for International Cooperation in Research and Higher Education (STINT), and the Swedish Foundation for Strategic Research (SSF).

References

Atanassov, I.I., Etchells, J.P., Turner, S.R., 2009. A simple, flexible and efficient PCR-fusion/Gateway cloning procedure for gene fusion, site-directed mutagenesis, short sequence insertion and domain deletions and swaps. Plant Methods 5, 14.
Bai, Y., McCoy, J.G., Levin, E.J., Sobrado, P., Rajashankar, K.R., Fox, B.G., Zhou, M., 2015. X-ray structure of a mammalian stearoyl-CoA desaturase. Nature 524, 252–256.
Beckmann, C., Rattke, J., Oldham, N.J., Sperling, P., Heinz, E., Boland, W., 2002. Characterization of a Δ8-sphingolipid desaturase from higher plants: a stereochemical and mechanistic study on the origin of *E,Z* isomers. Angew. Chem. Int. Ed. 41, 2298–2300.
Broadwater, J.A., Whittle, E., Shanklin, J., 2002. Desaturation and hydroxylation: residues 148 and 324 of *Arabidopsis* FAD2, in addition to substrate chain length, exert a major influence in partitioning of catalytic specificity. J. Biol. Chem. 277, 15613–15620.
Broun, P., Shanklin, J., Whittle, E., Somerville, C., 1998. Catalytic plasticity of fatty acid modification enzymes underlying chemical diversity of plant lipids. Science 282, 1315–1317.
Buser, H.R., Arn, H., Guerin, P., Rauscher, S., 1983. Determination of double bond position in mono-unsaturated acetates by mass spectrometry of dimethyl disulfide adducts. Anal. Chem. 55, 818–822.
Buček, A., Matoušková, P., Vogel, H., Šebesta, P., Jahn, U., Weißflog, J., Svatoš, A., Pichová, I., 2015. Evolution of moth sex pheromone composition by a single amino acid substitution in a fatty acid desaturase. Proc. Natl. Acad. Sci. U. S. A. 112, 12586–12591.
Cahoon, E.B., Lindqvist, Y., Schneider, G., Shanklin, J., 1997. Redesign of soluble fatty acid desaturases from plants for altered substrate specificity and double bond position. Proc. Natl. Acad. Sci. U. S. A. 94, 4872–4877.
Cahoon, E.B., Shanklin, J., Lindqvist, Y., Schneider, G., 1999. Modified Acyl-ACP desaturase. US 5888790 A.
Ding, B.J., Liénard, M.A., Wang, H.L., Zhao, C.H., Löfstedt, C., 2011. Terminal fatty-acyl-CoA desaturase involved in sex pheromone biosynthesis in the winter moth (*Operophtera brumata*). Insect Biochem. Mol. Biol. 41, 715–722.
Ding, B.J., Hofvander, P., Wang, H.L., Durrett, T.P., Stymne, S., Löfstedt, C., 2014. A plant factory for moth pheromone production. Nat. Commun. 5, 3353.
Gagné, S.J., Reed, D.W., Gray, G.R., Covello, P.S., 2009. Structural control of chemoselectivity, stereoselectivity, and substrate specificity in membrane-bound fatty acid acetylenases and desaturases. Biochemistry 48, 12298–12304.
Guy, J.E., Abreu, I.A., Moche, M., Lindqvist, Y., Whittle, E., Shanklin, J., 2006. A single mutation in the castor Delta9-18:0-desaturase changes reaction partitioning from desaturation to oxidase chemistry. Proc. Natl. Acad. Sci. U. S. A. 103, 17220–17224.
Guy, J.E., Whittle, E., Kumaran, D., Lindqvist, Y., Shanklin, J., 2007. The crystal structure of the ivy Δ4–16:0-ACP desaturase reveals structural details of the oxidized active site and potential determinants of regioselectivity. J. Biol. Chem. 282, 19863–19871.
Hao, G., O'Connor, M., Liu, W.T., Roelofs, W.L., 2002. Characterization of Z/E11- and Z9-desaturases from the obliquebanded leafroller moth, *Choristoneura rosaceana*. J. Insect Sci. 2, 26.
Hagström, Å.K., Wang, H.L., Liénard, M.A., Lassance, J.M., Johansson, T., Löfstedt, C., 2013. A moth pheromone brewery: production of (*Z*)-11-hexadecenol by heterologous co-expression of two biosynthetic genes from a noctuid moth in a yeast cell factory. Microb. Cell Fact. 12, 125.
Haritos, V.S., Horne, I., Damcevski, K., Glover, K., Gibb, N., 2014. Unexpected functional diversity in the fatty acid desaturases of the flour beetle *Tribolium castaneum* and identification of key residues determining activity. Insect Biochem. Mol. Biol. 51, 62–70.
Jeong, S.E., Rosenfield, C.L., Marsella-Herrick, P., You, K.M., Knipple, D.C., 2003. Multiple acyl-CoA desaturase-encoding transcripts in pheromone glands of *Helicoverpa assulta*, the oriental tobacco budworm. Insect Biochem. Mol. Biol. 33, 609–622.
Knipple, D.C., Rosenfield, C.L., Miller, S.J., Liu, W., Tang, J., Ma, P.W.K., Roelofs, W.L., 1998. Cloning and functional expression of a cDNA encoding a pheromone gland-specific acyl-CoA Δ11-desaturase of the cabbage looper moth, *Trichoplusia ni*. Proc. Natl. Acad. Sci. U. S. A. 95, 15287–15292.
Knipple, D.C., Rosenfield, C.L., Nielsen, R., You, K.M., Jeong, S.E., 2002. Evolution of the integral membrane desaturase gene family in moths and flies. Genetics 162, 1737–1752.
Krogh, A., Larsson, B., von Heijne, G., Sonnhammer, E.L., 2001. Predicting transmembrane protein topology with a hidden Markov model: application to complete genomes. J. Mol. Biol. 305, 567–580.
Lassance, J.M., Groot, A.T., Liénard, M.A., Antony, B., Borgwardt, C., Andersson, F., Hedenström, E., Heckel, D.G., Löfstedt, C., 2010. Allelic variation in a fatty-acyl reductase gene causes divergence in moth sex pheromones. Nature 466, 486–489.
Lassance, J.M., Liénard, M.A., Antony, B., Qian, S., Fujii, T., Tabata, J., Ishikawa, Y., Löfstedt, C., 2013. Functional consequences of sequence variation in the pheromone biosynthetic gene *pgFAR* for *Ostrinia* moths. Proc. Natl. Acad. Sci. U. S. A. 110, 3967–3972.
Liénard, M.A., Löfstedt, C., 2010. Functional flexibility as a prelude to signal diversity? Comm. Integr. Biol. 3, 586–588.
Liénard, M.A., Strandh, M., Hedenström, E., Johansson, T., Löfstedt, C., 2008. Key biosynthetic gene subfamily recruited for pheromone production prior to the extensive radiation of Lepidoptera. BMC Evol. Biol. 8, 270.

Liénard, M.A., Lassance, J.M., Wang, H.L., Zhao, C.H., Piskur, J., Johansson, T., Löfstedt, C., 2010. Elucidation of the sex-pheromone biosynthesis producing 5,7-dodecadienes in *Dendrolimus punctatus* (Lepidoptera: Lasiocampidae) reveals Δ11-and Δ9-desaturases with unusual catalytic properties. Insect Biochem. Mol. Biol. 40, 440–452.

Libisch, B., Michaelson, L.V., Lewis, M.J., Shewry, P.R., Napier, J.A., 2000. Chimeras of Δ6-fatty acid and Δ8-sphingolipid desaturases. Biochem. Biophys. Res. Commun. 279, 779–785.

Lindqvist, Y., Huang, W., Schneider, G., Shanklin, J., 1996. Crystal structure of Δ9 stearoyl-acyl carrier protein desaturase from castor seed and its relationship to other di-iron proteins. EMBO J. 15, 4081–4092.

Liu, W.T., Jiao, H.M., Murray, N.C., O'Connor, M., Roelofs, W.L., 2002. Gene characterized for membrane desaturase that produces (*E*)-11 isomers of mono- and diunsaturated fatty acids. Proc. Natl. Acad. Sci. U. S. A. 99, 620–624.

Liu, W.T., Rooney, A.P., Xue, B.Y., Roelofs, W.L., 2004. Desaturases from the spotted fireworm moth (*Choristoneura parallela*) shed light on the evolutionary origins of novel moth sex pheromone desaturases. Gene 342, 303–311.

Los, D.A., Murata, N., 1998. Structure and expression of fatty acid desaturases. Biochem. Biophys. Acta 1394, 3–15.

Löfstedt, C., Herrebout, W.H., Menken, S.B.J., 1991. Sex pheromones and their potential role in the evolution of reproductive isolation in small ermine moths (Yponomeutidae). Chemoecology 2, 20–28.

Löfstedt, C., Wahlberg, N., Millar, J.M., 2016. Evolutionary patterns of pheromone diversity in Lepidoptera. In: Allison, J.D., Cardé, R.T. (Eds.), Pheromone Communication in Moths: Evolution, Behavior and Application. University of California Press, Berkeley, pp. 43–77.

Man, W.C., Miyazaki, M., Chu, K., Ntambi, J.M., 2006. Membrane topology of mouse stearoyl-CoA desaturase 1. J. Biol. Chem. 281, 1251–1260.

Matoušková, P., Pichová, I., Svatoš, A., 2007. Functional characterization of a desaturase from the tobacco hornworm moth (*Manduca sexta*) with bifunctional *Z*11 and 10,12-desaturase activity. Insect Biochem. Mol. Biol. 37, 601–610.

Meesapyodsuk, D., Reed, D.W., Covello, P.S., Qiu, X., 2007. Primary structure, regioselectivity, and evolution of the membrane-bound fatty acid desaturases of *Claviceps purpurea*. J. Biol. Chem. 282, 20191–20199.

Meesapyodsuk, D., Qiu, X., 2014. Structure determinants for the substrate specificity of acyl-CoA Δ9 desaturases from a marine copepod. ACS Chem. Biol. 9, 922–934.

Moto, K., Suzuk, M.G., Hull, J.J., Kurata, R., Takahashi, S., Yamamoto, M., Okano, K., Imai, K., Ando, T., Matsumoto, S., 2004. Involvement of a bifunctional fatty-acyl desaturase in the biosynthesis of the silkmoth, Bombyx mori, sex pheromone. Proc. Natl. Acad. Sci. U. S. A. 101, 8631–8636.

Okuley, J., Lightner, J., Feldmann, K., Yadav, N., Lark, E., Browse, J., 1994. *Arabidopsis* FAD2 gene encodes the enzyme that is essential for polyunsaturated lipid synthesis. Plant Cell 6, 147–158.

Pinilla, A., Camps, F., Fabrias, G., 1999. Cryptoregiochemistry of the Δ11-myristoyl-CoA desaturase involved in the biosynthesis of *Spodoptera littoralis* sex pheromone. Biochemistry 38, 15272–15277.

Roelofs, W.L., Liu, W.T., Hao, G.X., Jiao, H.M., Rooney, A.P., Linn Jr., C.E., 2002. Evolution of moth sex pheromones via ancestral genes. Proc. Natl. Acad. Sci. U. S. A. 99, 13621–13626.

Schneiter, R., Tatzer, V., Gogg, G., Leitner, E., Kohlwein, S.D., 2000. Elo1p-dependent carboxy-terminal elongation of C14:Δ9 to C16:Δ11 fatty acids in *Saccharomyces cerevisiae*. J. Bacteriol. 182, 3655–3660.

Serra, M., Piña, B., Bujons, J., Camps, F., Fabriàs, G., 2006. Biosynthesis of 10,12-dienoic fatty acids by a bifunctional Δ11 desaturase in *Spodoptera littoralis*. Insect Biochem. Mol. Biol. 36, 634–641.

Serra, M., Piña, B., Abad, J.L., Camps, F., Fabriàs, G., 2007. A multifunctional desaturase involved in the biosynthesis of the processionary moth sex pheromone. Proc. Natl. Acad. Sci. U. S. A. 104, 16444–16449.

Shanklin, J., Whittle, E., Fox, B.G., 1994. Eight histidine residues are catalytically essential in a membrane-associated iron enzyme, stearoyl-CoA desaturase, and are conserved in alkane hydroxylase and xylene monooxygenase. Biochemistry 33, 12787–12794.

Shanklin, J., Cahoon, E., 1998. Desaturation and related modifications of fatty acids. Ann. Rev. Plant Physiol. Plant Mol. Biol. 49, 611–641.

Sperling, P., Ternes, P., Zank, T.K., Heinz, E., 2003. The evolution of desaturases. Prostaglandins Leukot. Essent. Fat. Acids 68, 73–95.

Tocher, D.R., Leaver, M.J., Hodgson, P.A., 1998. Recent advances in the biochemistry and molecular biology of fatty acyl desaturases. Prog. Lipid Res. 37, 73–117.

Trott, O., Olson, A.J., 2010. AutoDock Vina: improving the speed and accuracy of docking with a new scoring function, efficient optimization and multithreading. J. Comput. Chem. 31, 455–461.

Vanhercke, T., Shrestha, P., Green, A.G., Singh, S.P., 2011. Mechanistic and structural insights into the regioselectivity of an acyl-CoA fatty acid desaturase via directed molecular evolution. J. Biol. Chem. 286, 12860–12869.

Wang, H.L., Liénard, M.A., Zhao, C.H., Wang, C.Z., Löfstedt, C., 2010. Neofunctionalization in an ancestral insect desaturase lineage led to rare Δ6 pheromone signals in the Chinese tussah silkworm. Insect Biochem. Mol. Biol. 40, 742–751.

Wang, H., Klein, M.G., Zou, H., Lane, W., Snell, G., Levin, I., Li, K., Sang, B.C., 2015. Crystal structure of human stearoyl-coenzyme A desaturase in complex with substrate. Nat. Struct. Mol. Biol. 22, 581–585.

Whittle, E.J., Tremblay, A.E., Buist, P.H., Shanklin, J., 2008. Revealing the catalytic potential of an acyl-ACP desaturase: tandem selective oxidation of saturated fatty acids. Proc. Natl. Acad. Sci. U. S. A. 105, 14738–14743.